can be detected with an error of 0.016 km by this proposed method.

ACKNOWLEDGMENT

This work was supported by the Natural Science Foundation of Liaoning Province under Grant 201602262, the Fundamental Research Funds for the Central Universities under Grant N140405001 and N150401001, the National Science Foundation for Distinguished Young Scholars of China under Grant 61425003, the National Natural Science Foundation of China under Grant 51607028.

REFERENCES

[1] Su J. Study on Partial Discharge of High Voltage Power Cable. Unpublished doctoral dissertation, 2012; Dalian University of Technology, Dalian, China.

[2] Li HL, Li FX, Xu YM, Zhu HG. Partial discharge monitoring for cable terminals based on ultrasonic. *East China Electric Power*. 2008;3:011

[3] Du BX, Xing YQ, Jin JX, et al. Characterization of partial discharge with polyimide film in considering high temperature superconducting cable insulation. *IEEE Trans Appl Supercond*. 2014;24(5):1–5.

[4] Algeelani NA, Piah MAM, Iqbal SZ. (2013, June). Optical detection and evaluation of partial discharge on glass insulator. In: Power Engineering and Optimization Conference (PEOCO), 2013 IEEE 7th International, (pp. 87–91), IEEE.

[5] Zhiqiang Z, MacAlpine M. The directionality of an optical fiber high-frequency acoustic sensor for partial discharge detection and location. *J Lightwave Technol*. 2000;18(6):795.

[6] Wild G, Hinckley S. Acousto-ultrasonic optical fiber sensors: overview and state-of-the-art. *IEEE Sens J*. 2008;8(7):1184–1193.

[7] Pang B, Wu Y, Jia B, et al. A method for location the partial discharge: all-fiber interferometer location system. *Opt Instrum*. 2014;36(4):300–305.

[8] Li Z, Shen L, Ye X. Study of polarization-insensitive fiber optic Michelson interferometric sensors. *J Zhejiang Univ*. 2002;36(1): 44–46.

[9] Hang LJ, He CF, Wu B. A new pipeline leakage detection system based on linear optical fiber Sagnac interferometer and its location technology. *Chin J Lasers*. 2007;34(6):820

[10] Huang SC, Lin WW, Tsai MT, Chen MH. Fiber optic in-line distributed sensor for detection and localization of the pipeline leaks. *Sensor Actuator A Phys*. 2007;135(2):570–579.

How to cite this article: Song Z, Guo M, Wang Q. A partial discharge detection and localization system for high voltage cable based on long-tailed Sagnac interferometric fiber optic sensor. *Microw Opt Technol Lett*. 2017;59:2132–2136. https://doi.org/10.1002/mop.30692

Received: 8 February 2017

DOI: 10.1002/mop.30699

Design of a ceiling-mounted reader antenna to maximize the readable volume coverage ratio for an indoor UHF RFID application

J. Choo[1] | S. Yoo[2] | H. Choo[2]

[1] Department of Instrumentation, Control and Electrical System, Korea Institute of Nuclear Safety, Daejeon, South Korea

[2] School of Electronic and Electrical Engineering, Hongik University, Seoul, Korea

Correspondence
Hosung Choo, School of Electronic and Electrical Engineering, Hongik University, Seoul, Korea.
Email: hschoo@hongik.ac.kr

Abstract

We propose a novel ceiling-mounted reader antenna to achieve a specific readable volume for an indoor radio frequency identification (RFID) application. To satisfy various performances required for the indoor RFID application, a multilayered helix is adopted and optimized by a Pareto genetic algorithm in conjunction with a full-wave electromagnetic field simulator. The optimized antenna is fabricated, and the measured results show a matching bandwidth of 15.4%, a CP bandwidth of 6.5%, and a maximum gain of 4.3 dBic. When the fabricated antenna is installed on the ceiling, the measured readable volume for both horizontally and vertically placed tags at 912 MHz is over 4.7 m^3 out of the target volume of 9 m^3. Results verify that the proposed antenna is suitable for a reader antenna installed on ceiling in an indoor RFID application.

KEYWORDS

beam shape optimization, ceiling-mounted helix antenna, maximum readable volume coverage

1 | INTRODUCTION

Radio frequency identification (RFID) is an automatic detection system that obtains information about tags attached to objects using electromagnetic fields.[1] In order to improve the

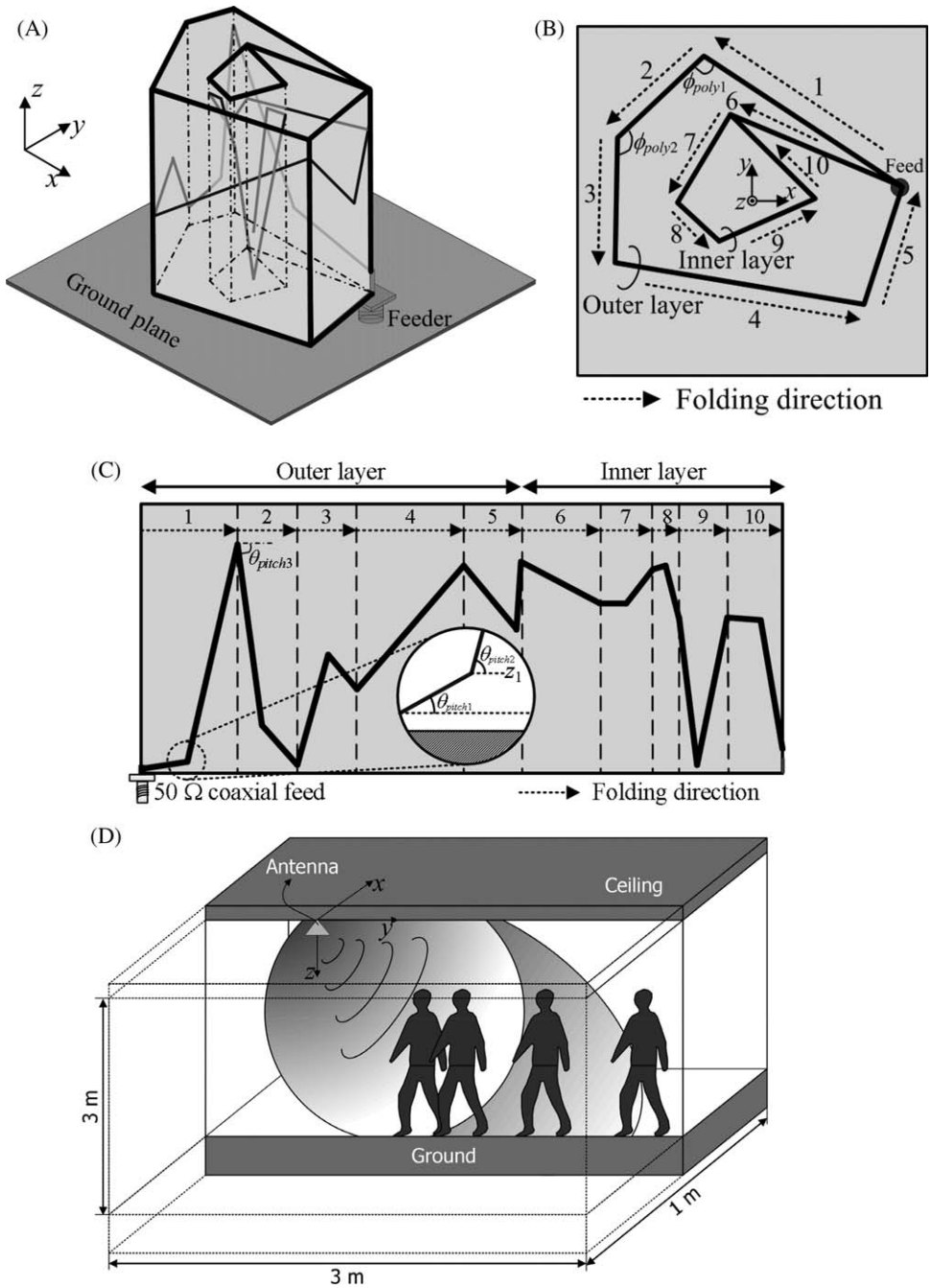

FIGURE 1 Geometry of the ceiling-mounted reader antenna. (A) 3-D view. (B) Top view. (C) Unfolded antenna body. (D) Mounting location on the ceiling and target volume in an indoor application

reading performance of RFID systems, extensive research on RFID in ultrahigh frequency band (UHF, 860–960 MHz) has been performed, such as the study of increasing the reading performances for reader and tag antennas,[2,3] a practical research of an indoor reader antenna focused on achieving a stable reading range,[4] and the study on the effects of indoor UHF electromagnetic fields on the human body.[5] In indoor environments, the most appropriate placement of the reader antenna is often considered as a ceiling because such placement directs the antenna toward the incoming target objects and makes the antenna avoid the interference from objects on the ground.[6] In addition, the ceiling-mounted reader antenna can extend the reading distance by using the ceiling as a large ground or a reflector.[7] The topics of most previous studies on ceiling-mounted antennas have been limited to radiation beam patterns with symmetric lobes, as reported in Refs. [8–10]. Nevertheless, such a symmetrical beam pattern may not guarantee an effective reading coverage for the intended area in an indoor environment.

In this paper, we propose a novel ceiling-mounted helix antenna with an optimized beam shape that covers a specific readable volume for indoor RFID applications. The antenna

should have a broad matching bandwidth to cover the UHF band in RFID with a low axial ratio. The antenna is then able to provide a specific readable volume where the tags should be detected by the reader, regardless of the tags' orientation. To satisfy the aforementioned design requirements, we use a full-wave electromagnetic field simulator, Numerical Electromagnetic Code (NEC),[11] in conjunction with a Pareto genetic algorithm (PGA)[12,13] for the beam shape optimization. The optimized antenna is fabricated using copper striplines on a flexible cardboard, and its measured performances are compared to those of the simulation. The results verify that the proposed antenna is suitable for a reader antenna installed on a ceiling in an indoor UHF RFID application.

2 | ANTENNA GEOMETRY

Figure 1A shows the geometry of the proposed antenna, which consists of a pentagonal outer layer and a quadrilateral inner layer. The folding shape of the layers is determined by folding angles (ϕ_{polyN}), as indicated in Figure 1B. Figure 1C illustrates the unfolded inner and outer layers where copper striplines are printed on a flexible cardboard ($\varepsilon_r = 2.3$, $\tan\delta = 0.022$) with pitch angles (θ_{pitchN}) and heights (z_N). The ϕ_{polyN}, θ_{pitchN}, and z_N values at the bent points complete the structure of the folded layers with the printed striplines, as shown in Figure 1A. Since the current distributions on the striplines are controlled by ϕ_{polyN}, θ_{pitchN}, and z_N, the values are carefully determined so that the antenna can achieve circularly polarized (CP) radiation characteristics. In particular, the stripline with the first folding angle (ϕ_{poly1}), pitch angle (θ_{poly1}), and height (z_1) determine a feeding structure in the outer layer, which is important in order to control the input impedance for a broad matching bandwidth.[14] The striplines are then extended to the inner layer, and the currents through the inner layer form an additional helix turn within the confined space to increase the overall antenna gain. Figure 1D shows the target volume for an indoor RFID application, where tags should be detected at 912 MHz by the reader, regardless of the tags' orientation. ϕ_{polyN}, θ_{pitchN}, and z_N are determined so that the antenna produces an appropriate beam shape in the radiation pattern to maximize the reading performance at the target volume. The antenna should have a broad matching bandwidth to cover the entire UHF RFID frequency band and should exhibit the CP characteristic with a low axial ratio. To obtain the optimum ϕ_{polyN}, θ_{pitchN}, and z_N values that satisfy the specifications, we use an optimization algorithm of the PGA in conjunction with a full wave electromagnetic field simulator NEC that is efficient for analyzing wire-shaped antennas. The four cost functions used in the PGA process are listed as follows:

$$\text{Cost } 1 = 1 - \frac{1}{2}\left(\frac{\text{Eff}_{\text{Reader}} \times \text{BW}_{\text{Reader}}}{\text{BW}_{\text{RFID}}} + \text{RQ}\right) \quad (1)$$

$$\text{Cost } 2 = 1 - \frac{1}{2}\left(\frac{\text{CPBW}_{\text{Reader}}}{\text{BW}_{\text{RFID}}} + \text{AQ}\right) \quad (2)$$

$$\text{Cost } 3 = \frac{kr_{\text{Reader}}}{kr_{\text{RFID}}} \quad (3)$$

$$\text{Cost } 4 = 1 - \text{RCR} = 1 - \frac{\text{RV}_{\text{Reader}}}{\text{RV}_{\text{RFID}}}, \quad (4)$$

where

$$\text{RQ} = \begin{cases} 0 & , \text{ if } \text{Eff}_{\text{Reader}} \times \text{BW}_{\text{Reader}} \le \text{BW}_{\text{RFID}} \\ \dfrac{\text{RL}_{\text{RFID}} - \text{RL}_{\text{Max}}}{\text{RL}_{\text{RFID}}} & , \text{ if } \text{Eff}_{\text{Reader}} \times \text{BW}_{\text{Reader}} > \text{BW}_{\text{RFID}} \end{cases}$$

$$\text{AQ} = \begin{cases} 0 & , \text{ if } \text{CPBW}_{\text{Reader}} \le \text{BW}_{\text{RFID}} \\ \dfrac{\text{AR}_{\text{RFID}} - \text{AR}_{\text{Max}}}{\text{AR}_{\text{RFID}}} & , \text{ if } \text{CPBW}_{\text{Reader}} > \text{BW}_{\text{RFID}} \end{cases}.$$

Cost 1 is calculated using the product of the radiation efficiency ($\text{Eff}_{\text{Reader}}$) and the matching bandwidth ($\text{BW}_{\text{Reader}}$) of sample antennas in the PGA process where BW_{RFID} is the frequency band required for UHF RFID (860–960 MHz). When $\text{BW}_{\text{Reader}} \times \text{Eff}_{\text{Reader}}$ is greater than BW_{RFID}, the reflection coefficient quality (RQ) is added to the cost function to reduce the reflection coefficient to a value less than a reference matching condition of −10 dB ($\text{RL}_{\text{RFID}} = -10$ dB). *Cost* 2 is calculated by the CP bandwidth ($\text{CPBW}_{\text{Reader}}$) in the direction of the main lobe. Similarly, the axial ratio quality (AQ) is added to the cost function to reduce the axial ratio to a value less than 3 dB ($\text{AR}_{\text{RFID}} = 3$ dB). *Cost* 3 is the ratio of the electrical size of the sample antennas ($\text{kr}_{\text{Reader}}$) to an allowable electrical size ($\text{kr}_{\text{RFID}} = 3.3$), where k is a wave number at 912 MHz and r is the radius of the sphere that encloses the helix antenna structure. In *Cost* 4, the reading coverage ratio (RCR) is obtained using the Friss transmission equation.[15] The *RCR* is defined as the ratio of the readable volume ($\text{RV}_{\text{Reader}}$) to the target volume RV_{RFID} (1 m × 3 m × 3 m), where both horizontally and vertically oriented tags are detected by the reader with an input power of 1 W.

3 | RESULTS

After the PGA process, the optimized sample antennas residing at the Pareto front are obtained. One of the optimized samples at the Pareto front is chosen, and the geometric information in the Cartesian coordinate (x, y, z) corresponding to ϕ_{polyN}, $\theta_{pitchN,}$ and z_N at bent points is listed in Table 1. The optimized sample antenna (size, $kr = 3.08$) shows a matching bandwidth of 8.7%, a CP bandwidth of 9.1%, and an *RCR* of 0.65 (65%). The antenna is then fabricated by

TABLE 1 Design parameters for the proposed antenna

Parameters	Value
Bent point	Position (mm)
Feeder	(67, 0, 3)
Point 1	(32, 32, 8)
Point 2	(–6, 37, 146)
Point 3	(–26, 55, 30)
Point 4	(–58, 35, 6)
Point 5	(–60, 5, 76)
Point 6	(–62, −27, 53)
Point 7	(28, −49, 122)
Point 8	(42, −53, 132)
Point 9	(66, −3, 90)
Point 10	(67, 0, 135)
Point 11	(–5, 34, 108)
Point 12	(–18, 9, 108)
Point 13	(–31, −15, 129)
Point 14	(–22, −22, 133)
Point 15	(–10, −32, 101)
Point 16	(6, −23, 5)
Point 17	(33, −7, 99)
Point 18	(12, 16, 98)
Point 19	(–5, 34, 12)

folding a flexible cardboard ($\varepsilon_r = 2.3$, $\tan\delta = 0.022$, thickness = 2 mm) where the copper striplines are printed on the cardboard (line width = 2 mm), and it is mounted on a circular ground plane with a diameter of 0.3 m for measurements in an anechoic chamber. Figures 2 and 3 show the reflection coefficient and the axial ratio as a function of frequency. The measured matching and CP bandwidths are 15.4% (865–1005 MHz) and 6.5% (861–920 MHz), respectively. The measured CP bandwidth is observed in the maximum measured gain direction of $\theta = 26°$ and $\phi = 90°$ while the simulated CP bandwidth is calculated in the maximum simulated gain direction of $\theta = 63°$ and $\phi = 90°$. The maximum gain direction of the measurement is shifted by about 30° compared to the simulated results, and such deviations are caused by the dielectric constant of the cardboard and the finite ground plane, which are not considered in NEC simulations. Figure 4A shows the measured radiation patterns on the *x*-*z* ($\phi = 0°$) plane, and the radiation pattern of the RHCP gain

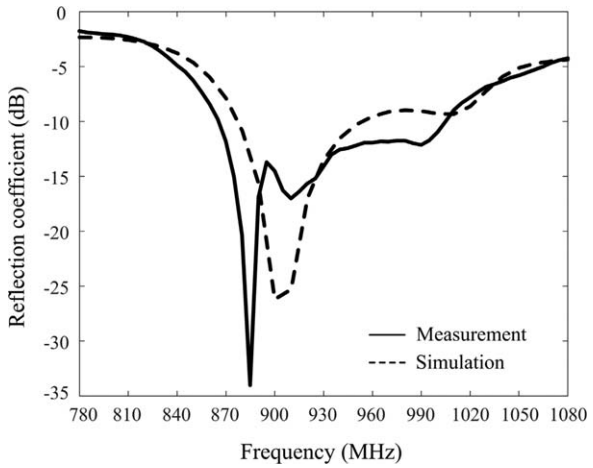

FIGURE 2 Measured and simulated reflection coefficients

exhibits a particularly wide beam width of 66° with a maximum gain of 2.1 dBic at $\theta = 0°$, which allows the reader antenna to have a large readable volume. The radiation pattern of the RHCP gain on the *y*-*z* ($\phi = 90°$) plane shown in Figure 4B, is tilted to $\theta = 26°$ and $\phi = 90°$ to optimally cover the target volume. Note that the maximum gain value of 4.3 dBic with a beam width of 50.4° is observed at $\theta = 26°$ and $\phi = 90°$ in *y*-*z* plane, and a right-hand circular polarization in the main beam direction is observed with a cross polarization level of −15.4 dB. These results demonstrate that the proposed antenna has a proper beam shape to achieve an optimum reading characteristics for a given target volume. Figure 5 shows the measured maximum reading distances along the *z*-axis on the *x*-*y* plane in the target volume (see Figure 1D). The measured reading distances at 912 MHz are plotted separately in accordance with the orientation of the tag. The designed reader antenna is mounted on a ceiling of origin ($x = 0$ mm, $y = 0$ mm, $z = 0$ mm) and connected to a commercial reader system with an output power of 1 W.[16]

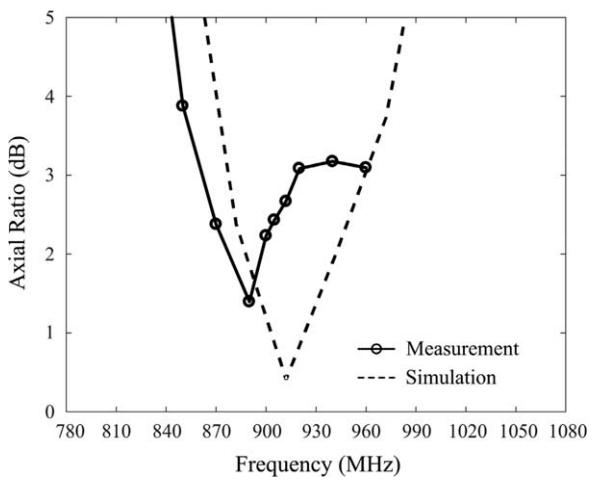

FIGURE 3 Measured and simulated axial ratios

Figures 5A,B show the results when the tag orientations are parallel to the *x*-axis (horizontal polarization) and parallel to the *z*-axis (vertical polarization), respectively. The readable volume of the horizontally oriented tags are about twice that of vertically oriented tags due to the radiation characteristics of the reader antenna. Figure 5C shows the stable reading area where both vertically and horizontally oriented tags can be detected. The results show the ratio of readable volume to the target volume (1 m × 3 m × 3 m) exceeding 52% (4.7 m^3) at 912 MHz. This verifies that the proposed antenna is suitable for ceiling-mounted antennas in an indoor RFID application.

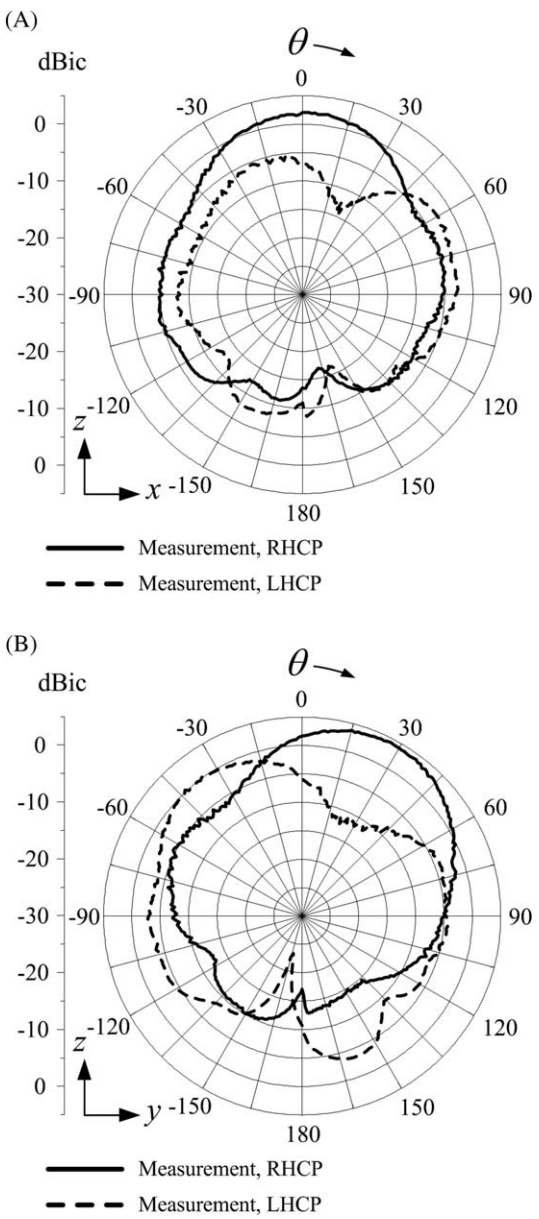

FIGURE 4 Radiation pattern of the proposed antenna at 912 MHz. (A) Measured radiation pattern in the *x*-*z* plane. (B) Measured radiation pattern in the *y*-*z* plane

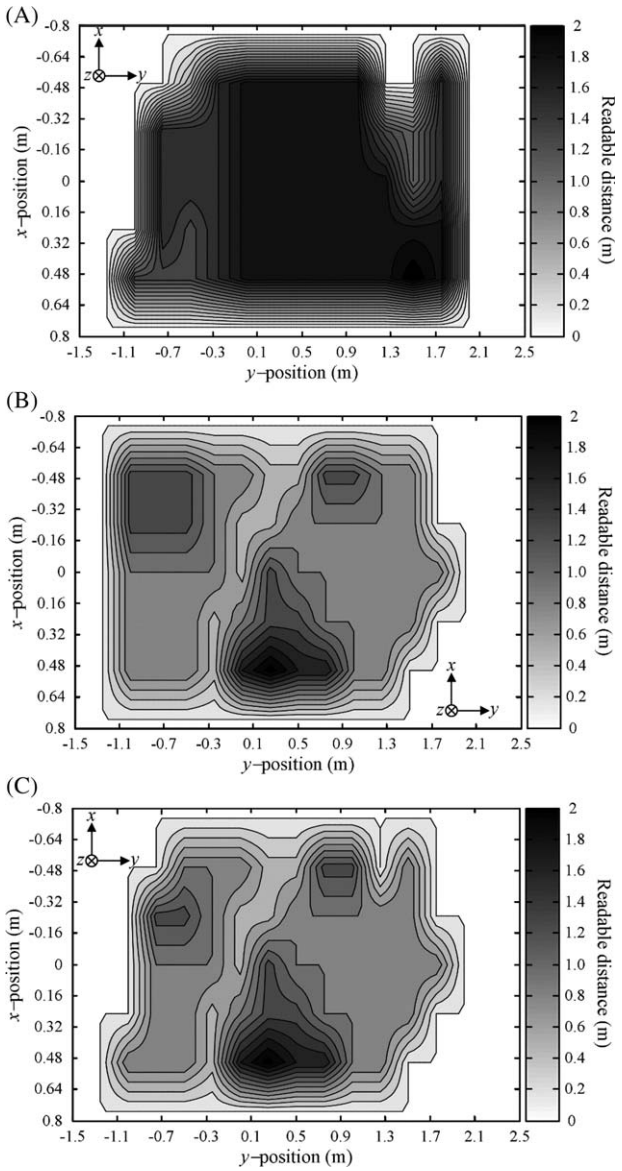

FIGURE 5 Measured reading distance in the target volume. (A) Measured reading distance for horizontally oriented tags. (B) Measured reading distance for vertically oriented tags. (C) Measured reading distance for both horizontally and vertically oriented tags

4 | CONCLUSIONS

To obtain a specific readable volume in an indoor RFID application, a ceiling-mounted reader antenna using a multilayered helix was proposed. To optimize the complicated antenna structure, the PGA based optimization process was employed in conjunction with the NEC EM simulator. The fabricated antenna with a size of $kr = 3.08$ showed a matching bandwidth of 15.4%, a CP bandwidth of 6.5%, and a maximum gain of about 4.3 dBic. In an indoor environment, the readable volume was then measured after mounting the antenna on a ceiling with a commercial reader system. The results showed a ratio of 52% readable volume (4.7 m^3) to target readable volume at 912 MHz, which verifies that the

proposed antenna is suitable for ceiling-mounted antennas in an indoor RFID application.

ACKNOWLEDGMENTS

This work was supported by the Korea Institute of Nuclear Safety under the project "Development of Proof Test Model and Safety Evaluation Techniques for the Regulation of Digital I&C Systems used in NPPs" (No. 1305003-0315-SB130) and the Basic Science Research Program through the National Research Foundation of Korea (NRF) funded by the Ministry of Education (No. 2015R1A6A1A03031833).

REFERENCES

[1] Dobkin DM. The RF in RFID: passive UHF RFID in practice. *Newnes*. 1997.

[2] Choo J, Cho C, Choo H. Three label tags for special applications: attaching on small targets, long distance recognition, and stable performance with arbitrary objects. *IEICE Trans Commun*. 2014;E97-B:1022–1029.

[3] Abbak M, Tekin I. RFID coverage extension using microstrip patch antenna array. *IEEE Trans Antennas Propag Mag*. 2009; 51:185–191.

[4] Dimitriou AG, Bletsas A, Sahalos JN. Room-coverage improvements in UHF RFID with commodity hardware. *IEEE Trans Antennas Propag Mag*. 2011;53:175–194.

[5] Kim H, Lee Y, Lee Y, et al. Effects of 915 MHz radio frequency identification electromagnetic field exposure on neuronal precursor cells in the dentate gyrus of adult rat brains. *J Electromagn Eng Sci*. 2015;15:173–180.

[6] DiGiamp E, Martinelli F. Mobile robot localization using the phase of passive UHF-RFID signals. *IEEE Trans Indus Electron*. 2014;61:365–376.

[7] Kishk AA, Shafai L. Gain enhancement of antennas over finite ground plane covered by a dielectric sheet. *IEE Proc*. 1987;134: 60–64.

[8] Pan Y, Leung KW. Wideband circularly polarized dielectric bird-nest antenna with conical radiation pattern. *IEEE Trans Antennas Propag Mag*. 2013;61:563–570.

[9] J-SR, Chan M-C. Reconfigurable circularly-polarized patch antenna with conical beam. *IEEE Trans Antennas Propag Mag*. 2010;58:2753–2757.

[10] Choo J, Choo H, Park I, Oh Y. Design of multi-layered polygonal helix antennas for RFID applications. *Microwave Opt Technol Lett*. 2007;49:1971–1974.

[11] Numerical Electromagnetics Code, NEC. http://www.nec2.org; 2016.

[12] Goldberg D. *Genetic Algorithms in Search, Optimization and Machine Learning*. New York: Wiley; 1989.

[13] Rahmat-Samii Y, Michielssen E. *Electromagnetic Optimization by Genetic Algorithms*. New York: Wiley; 1999.

[14] Johnson R, Cotton R. A backfire helical feed. *IEEE Trans Antennas Propag*. 1984;32:1126–1128.

[15] Balanis CA. *Antenna Theory Analysis and Design*. New York: Wiley; 1997.

[16] Alien technology, RFID system. http://www.alientechnology.com, 2017.

How to cite this article: Choo J, Yoo S, Choo H. Design of a ceiling-mounted reader antenna to maximize the readable volume coverage ratio for an indoor UHF RFID application. *Microw Opt Technol Lett*. 2017;59:2136–2141. https://doi.org/10.1002/mop.30699

Received: 17 February 2017

DOI: 10.1002/mop.30691

Two layer reconfigurable coaxial-fed antenna for S-band and GPS applications

L. Asadpor | **F. Nazari**

Department of Electrical Engineering, Urmia Branch, Islamic Azad University, Urmia, Iran

Correspondence
L. Asadpor, Department of Electrical Engineering, Urmia Branch, Islamic Azad University, Urmia, Iran.
Email: L.asadpour@iaurmia.ac.ir

Abstract

In this paper, a new design is introduced for variable-slot antennas. The proposed antenna structure is based on the slots placed in the edges of the patch and in the center of the patch. Then, using pin diodes this structure is converted into a variable antenna. It is worth noting that in this paper short-circuit and open-circuit structures are used instead of pin diodes. The two-band or multi-band structures studied in this paper are suitable for covering 1.82/2.71/2.82, 1.56/1.81/2.29/2.85, GPS, S, and GSM frequency bands.

KEYWORDS

pin diodes, slot antennas, variable antennas

1 | INTRODUCTION

Due to the fast expansion of satellite communication, multi-frequency, multi-function antennas are widely required in